Clays and Clay Minerals, Vol. 44, No. 5, 693–705, 1996.

CLAY MINERAL DIAGENESIS AND THERMAL HISTORY OF THE THONEX WELL, WESTERN SWISS MOLASSE BASIN

ROLAND SCHEGG[1,2] AND WERNER LEU[2]

[1] Département de Géologie et Paléontologie, 13 rue des Maraîchers, 1211 Geneva 4, Switzerland
[2] Geoform Ltd, Anton-Graff-Str. 6, 8401 Winterthur, Switzerland

Abstract—Results are presented of a diagenetic study from the 1300 m thick Oligocene Molasse deposits penetrated by the Thônex geothermal exploration well (Geneva, Switzerland). The x-ray diffraction (XRD) studies of fine-grained rocks indicate the following diagenetic changes: a decrease of illite/smectite (I/S) expandability from approximately 90% to 30% with depth, a decrease of the amount of I/S in the clay mineral fraction, and the appearance of corrensite at depths >750 m. The transition from random I/S to ordered I/S occurs at the base of the Thônex well (1200 to 1300 m) and is associated with a coal rank of about 0.7% Rr (mean random vitrinite reflectance) corresponding to paleotemperatures of 110 to 115 °C. Corrensite appears at a vitrinite reflectance value of 0.6% Rr and a corresponding paleotemperature of 100 °C. The amount of post-Molasse erosion is estimated to be approximately 2 km. Thermal history modeling of the Thônex well suggests maximum paleotemperatures of 80 to 115 °C and an average paleogeothermal gradient of 27 °C/km during Late Miocene maximum burial conditions.

Key Words—Chlorite/Smectite, Corrensite, Diagenesis, Erosion estimate, Illite/Smectite, Paleotemperatures, Thermal modeling, Vitrinite reflectance, XRD.

INTRODUCTION

Modern numerical basin modeling tools in hydrogeological and petroleum exploration studies requires a temporally continuous quantification of the burial and uplift history and a comprehensive set of thermal calibration data. Both organic and mineral indicators have been used to quantify diagenesis.

Vitrinite reflectance, Tmax from Rock-Eval pyrolysis, Thermal Alteration Index (TAI) or biomarkers are probably the most widely used thermal maturity indicators (Tissot et al. 1987). The development of kinetic models of vitrinite reflectance evolution based on viable chemical principles provide a powerful tool for thermal modeling (Larter 1989; Sweeney and Burnham 1990). Other studies dealing with changes in clay mineralogy in sedimentary rocks have tried to use mineral indicators to constrain the thermal history of sedimentary basins (Kübler 1973; Hoffman and Hower 1979; Smart and Clayton 1985; Pollastro and Barker 1986; Kisch 1987; Pearson and Small 1988; Pollastro 1993; Renac and Meunier 1995).

In the Swiss Molasse Basin, the disappearance of smectite with depth is associated with the formation of interstratified clay minerals (Monnier 1982). Two pathways of smectite transformations have been emphasized by this author, one toward an irregular 2:1 mixed-layer mineral (I/S), the other toward corrensite. Based on a review of coalification data, Teichmüller and Teichmüller (1986) posulated low paleogeothermal gradients for the Bavarian part of the Molasse Basin. According to these authors, the observed decrease of the coalification gradient (0.09 to 0.03% Rr/km) in boreholes of the South German Molasse toward the south is caused by a decrease of the geothermal gradient (from 30 to 20 °C/km) in the same direction. More recent studies in Switzerland by Rybach (1984), Schegg (1994) and Jenny et al. (1995) support this conclusion.

Our paper presents the results of a diagenetic study of the Tertiary Molasse deposits in the Thônex geothermal exploration well (Geneva, Switzerland). The well was drilled in 1993 and preliminary results have been reported by Jenny et al. (1995). We have chosen this well for an integrated study because of its simple burial history, for example, its burial and subsequent uplift/erosion, the well-defined geological and geodynamic framework and its good coalification profile. The main purposes of this study are to describe the clay mineral diagenesis, its comparison to the coalification evolution and the combined use of organic and inorganic maturity indicators for thermal history modeling.

GEOLOGICAL SETTING

The study area is situated in the western part of the Swiss Molasse Basin (Figure 1), a typical peripheral foreland basin overlying thickened lithosphere (Pfiffner 1986). The basin-fill is dominated by detrital deposits derived from the rising Alps. The Molasse sequence comprises 2 large coarsening and shallowing upward cycles separated by the Burdigalian unconformity. The succession is divided into 4 lithostratigraphic groups: 1) Lower Marine Molasse (UMM, Rupelian–Chattian), 2) Lower Freshwater Molasse (USM, Rupelian–?Burdigalian), 3) Upper Marine Molasse (OMM, Burdigalian–?Langhian) and 4) Upper Freshwater Molasse (OSM, Langhian–Serravalian).

Subsequent to the deposition of the continental OSM, the Molasse Basin was uplifted and its basin-

Copyright © 1996, The Clay Minerals Society

https://doi.org/10.1346/CCMN.1996.0440513 Published online by Cambridge University Press

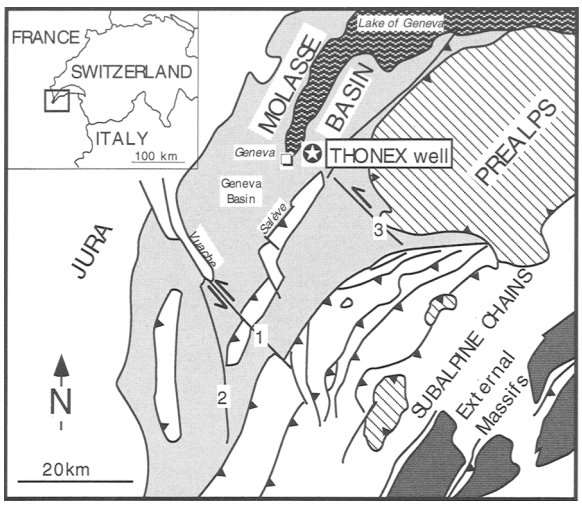

Figure 1. Tectonic map of the Haute-Savoie (France) and the Geneva Basin (Switzerland) modified after Wildi & Huggenberger (1993). 1: Vuache-Forens-Les Bouchoux strike-slip fault zone; 2: Alby fault; 3: Arve strike-slip fault zone.

fill partially eroded. This is well expressed on the present-day outcrop map of the Swiss Molasse Basin where from east to west erosion has cut progressively deeper. These field observations have been supported by diagenetic and geodynamic studies (Laubscher 1974; Lemcke 1974; Monnier 1982; Schegg 1992, 1993, 1994). The estimated missing section of the Thônex well location ranges from 1700 to 2300 m (Jenny et al. 1995).

The Thônex well is located in the Geneva Basin, which is bound by the first ridge of the Jura Mountains to the north and by the thrusted anticline of the Mount Salève to the south (Figure 1). Mesozoic sediments within this basin form a south-easterly dipping monocline with karstified Urgonian (Early Cretaceous) carbonates at the top (Gorin et al. 1993). NNW-SSE trending wrench faults, subparallel to the Vuache fault zone, cut the entire Geneva Basin (Gorin et al. 1993).

The Molasse sediments in the Geneva Basin consist only of USM which can be subdivided into the Molasse rouge and the Molasse grise ranging in age from late early Chattian to early Aquitanian (Berger et al. 1987). The thickness of USM strata decreases toward the NW, from over 1000 m near the Salève to zero close the Jura mountains.

METHODS

Whole Rock and Clay Mineral Analyses

Cuttings from the Tertiary USM were sampled at ≈60 m intervals from 84 m and down to 1317 m depth (Figure 2). Twenty-one samples of the fine-grained sedimentary succession (marls, siltstone and fine sandstone) were analyzed by XRD. Drill cuttings represent an "average" sample and tend to reduce the bed-to-bed variation.

The XRD analyses were performed at the University of Neuchâtel, by Prof. B. Kübler, using a SCINTAG XRD 2000 diffractometer operating at 45 kV and 40 mA using Cu-Kα radiation. The resulting digital data were processed for background correction. Samples were scanned in air-dried natural conditions and after saturation wth ethylene glycol (EG) from 1 to 50 °2θ at a scanning speed of 1 °/min. Calcerous rocks were decarbonated using a non-complexing, non-oxidizing acid (HCl). Oriented carbonate-free clay aggregates of the 2 to 16 μm and <2 μm fraction have been used for the XRD analysis.

Randomly oriented powders of the bulk sample have been used for characterization of the whole-rock mineralogy. The bulk rock mineralogy was estimated semi-quantitatively using external standards.

The relative proportion of clay minerals present in the <2 μm fraction was determined using the intensities of the following XRD peaks, after decomposition: (001/001) of I/S, (002) of corrensite (corr), (001/001) of chlorite/smectite (C/S), (001) of illite (ill), (002) of chlorite (chl) and (001) of kaolinite (kao). This method gives the relative proportion of the clay minerals normalized to 100%.

The partial overlapping of characteristic peaks of kaolinite, chlorite and mica with interstratified phases makes it difficult to separate the different contributions to the experimental XRD peaks. The problem of interfering XRD peaks exists over the entire angular range. We used the decomposition program of the SCINTAG 2000 software (SCINTAG™ 1992) to deconvolute the XRD peaks in the 1 to 30 °2θ range of the <2 μm fraction. This software fits the experimental XRD pattern with elementary curves that are assumed to be related to the different mineral phases present in the sample. For pattern fitting, the number of elementary curves, usually set by the user, has been kept as small as possible. Because pattern decomposition has only a physical meaning if the modeled phases correspond to phases that actually exist in the sediment, modeled elementary curves have been compared to and identified with simulated XRD patterns of different interstratified clay minerals (I/S and C/S). We used Reynolds NEWMOD (Reynolds 1985) program, which is included in the SCINTAG 2000 software (SCINTAG™ 1992).

We used the approach of Moore and Reynolds (1989) for estimating the percentage of smectite layers in I/S. Despite the ongoing debate on the nature of interlayering in the smectite-to-chlorite transformation (Shau et al. 1990; Hillier 1995), we based our interpretations on the smectite-chlorite mixed-layer model. We used the (002/002) and (004/005) peaks, and their angular difference to estimate the composition of C/S mixed-layer minerals (Moore and Reynolds 1989).

Thermal Modeling

The numerical simulation of a sedimentary basin on the basis of heat flow enables the determination of an

https://doi.org/10.1346/CCMN.1996.0440513 Published online by Cambridge University Press

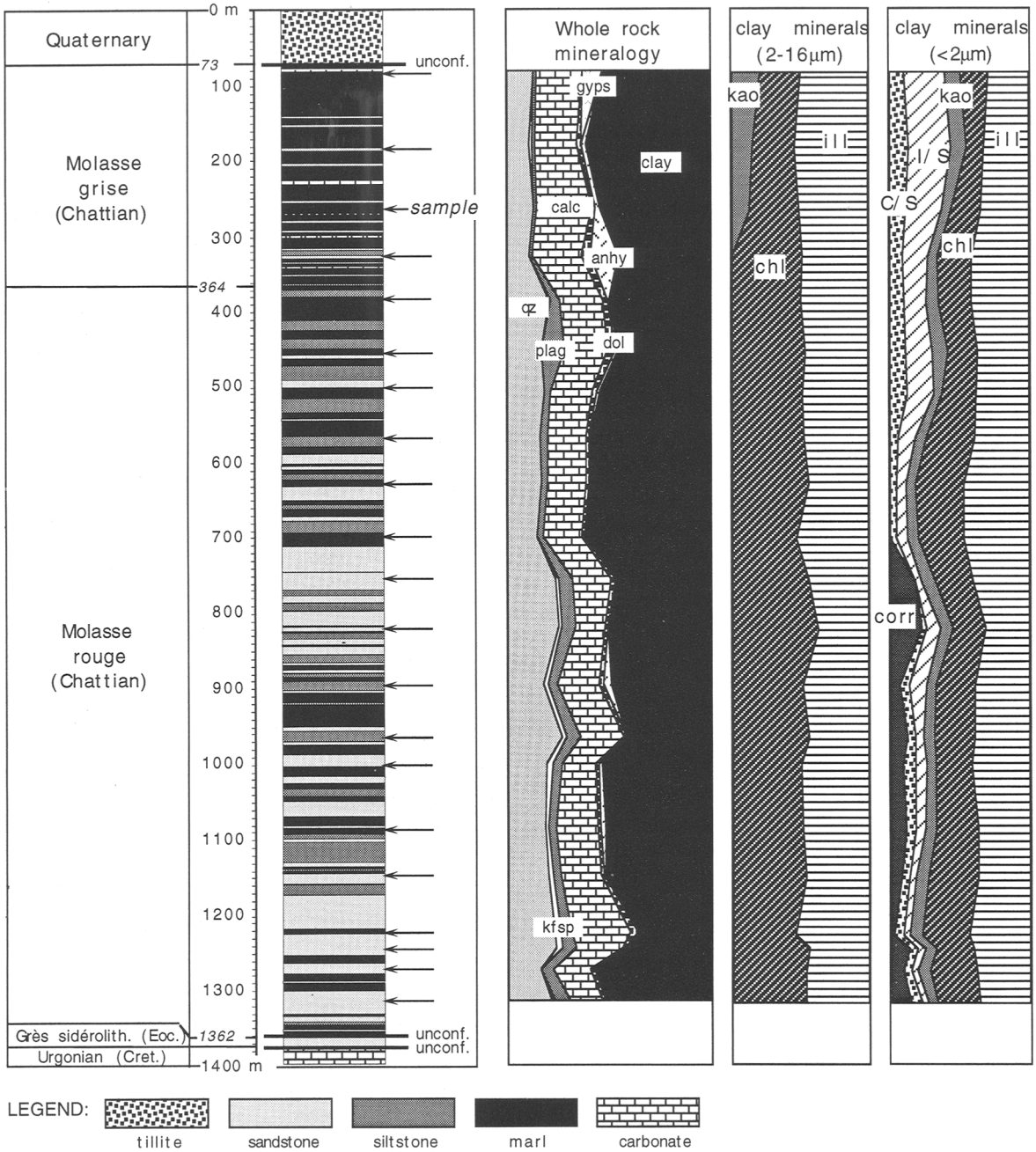

Figure 2. Lithostratigraphic, lithological and mineralogical profiles in the Tertiary section of the Thônex well. Arrows indicate sample location.

accurate temperature history by integrating factors that control temperatures and by calibrating with thermal indicators. A one-dimensional burial history model is used to provide a framework for modeling the thermal history of the Thônex well. The modeling was carried out using the BasinMod® program (Platte River Association, Version 4.0).

The following principle processes and parameters that control temperatures in a sedimentary basin are taken into account: 1) basic geological processes, for

https://doi.org/10.1346/CCMN.1996.0440513 Published online by Cambridge University Press

example, deposition, non-deposition and erosion; 2) boundary conditions, such as, heat flow history at the base and variation of the sediment/water interface temperatures at the top; and 3) petrophysical properties of each lithology, that is, thermal conductivity, heat capacity and compaction parameters.

Starting with a set of primary input values, parameters which have the most direct effect on the thermal history (heat flow at the base, amount of missing section) are changed until a good fit between measured and calculated calibration data is obtained. The relative importance of each thermo-physical parameter and the effects of changing geodynamic scenarios, for example, high, low or variable heat flow history, are addressed during the sensitivity analysis.

WHOLE-ROCK MINERALOGY

The lithology of the USM in the Thônex well (Figure 2) is dominated by fine-grained, argillaceous rocks, such as, marls, siltstones and fine-grained sandstones. The average composition of the Thônex well samples is as follows: quartz (18%), K-feldspar (1%), plagioclase (5%), calcite (21%), dolomite (2%), gypsum (1%), anhydrite (2%) and clay minerals (50%). The calculated amounts of calcite have been confirmed by direct determination of the calcite content on the drill site. The available mineralogical data show no systematic increase or decrease in the abundance of any of the non-clay mineral phases with depth.

MINERALOGY OF THE FINE FRACTION (<2 μm, 2 to 16 μm)

The fine-fraction of the carbonate-free clay samples is dominated by mica and chlorite, and minor amounts of kaolinite, mixed-layer I/S, mixed-layer C/S and corrensite (Figures 2 and 3). Quartz, K-feldspar and plagioclase are present in most samples with no apparent depth trend.

Illite and Illite/Smectite Mixed-layers

Illite is always present in both the <2 μm and the 2 to 16 μm size fractions. The integral 10 Å periodicity, regardless of sample treating of the (001) reflection at 9.95 to 9.99 Å, the (002) reflection at 4.98 to 5.0 Å, the (003) reflection at 3.32 to 3.33 Å, the (004) reflection at 2.49 Å and the (005) reflection at 1.99 Å documents its discrete character. The relative proportion of illite varies between 30 and 50% for the <2 μm fraction and between 40 and 50% for the 2 to 16 μm fraction, but no obvious depth trend can be observed (Figure 2). Ternary intensity diagrams of the harmonic series (001) of mica reflections can be used to define fields relating to a specific chemical composition (Rey and Kübler 1983). The samples studied plot in a field between illite and phengite.

The I/S phase is an important component of the <2 μm fraction, especially in the upper part of the well (up to 30%). The relative proportion of I/S decreases toward the base of the studied section (Figure 2). The asymmetric and broadened peaks of mica and chlorite in the 2 to 16 μm fraction indicate that I/S and/or C/S are probably present in small amounts. As no decomposition procedure was performed on this size fraction, the relative proportion of mixed-layer minerals has not been quantified.

The decomposition results of the complex XRD patterns (<2 μm fraction) in the 8 to 10 Å and the 5 to 6 Å angular regions (Figure 4) might be interpreted as a multi-phase I/S asemblage (4 I/S populations with different expandabilities) in the Molasse rocks. However, we are aware that such results may be strongly biased by the operator, especially when dealing with multiple low intensity peaks of such a complex mixture of clay minerals. Furthermore, I/S patterns calculated with NEWMOD suggest that any 2 corresponding I/S peaks, in terms of composition, which occur in the 8 to 10 Å and 5 to 6 Å angular regions should have about equal intensities. Figure 4 illustrates that this is not the case for our decomposed peaks. For these reasons, we have chosen a more classical interpretation approach by considering only one I/S phase.

The I/S shows a compositional trend with depth (Figures 3 and 8). Samples in the upper part of the well contain approximately 70 to 90% expandable layers, whereas samples at the base of the USM contain about 30 to 50% expandable layers. The decrease of the expandability of I/S seems to follow some linear trend, even when the variation of individual results is considered. The narrow variation with depth of the (001/001) reflection (at about 5.2 °2θ, 16 to 17 Å) indicates random interstratification (R = 0) throughout the studied section. However, the overall decrease of its intensity confirms a change in composition of a randomly interstratified mixed-layer (a similar trend has been modeled with NEWMOD).

Chlorite

Chlorite is ubiquitous in both size fractions. The relative proportion varies between 10 and 30% in the <2 μm fraction and between 30 and 60% in the 2 to 16 μm fraction (Figure 2). No significant depth trends could be observed.

Chlorite/Smectite and Corrensite

The presence of the following peaks after glycolation indicate the presence of a chlorite-rich mixed-layer: C/S (001/001) at 14.7 to 15.4 Å, C/S (002/002) at 7.2 to 7.5 Å and C/S (004/005) at about 3.5 Å (Figures 3 and 4). The estimated percentage of smectite in C/S varies between 10 and 35%. There is only a slight vertical variation for this phase, indicated by a restricted compositional variation (10 to 25% S in C/S) in the basal part of the studied section (1100 to 1400 m).

https://doi.org/10.1346/CCMN.1996.0440513 Published online by Cambridge University Press

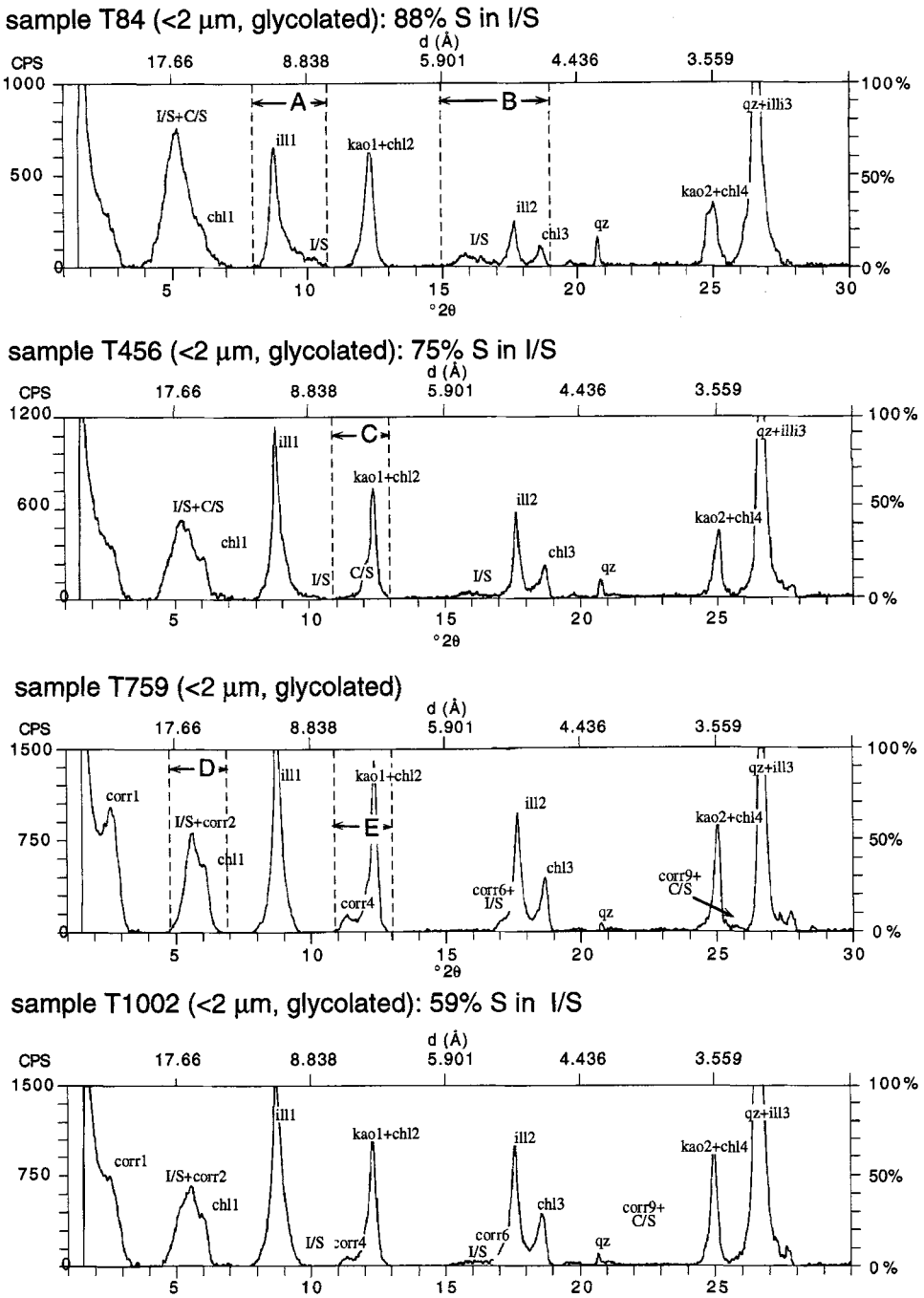

Figure 3. XRD patterns of four samples illustrating the clay mineral assemblages and estimates of I/S expandability. Note that the sample number corresponds to the sample depth. A–E: intervals for which deconvolution results are shown in Figure 4. Key: ill1, ill2, ill3 = basal spacing of illite: IISI = low epandable illitic phase; chl1, chl2, chl3, chl4 = basal spacing of chlorite; kao1, kao2 = basal spacing of kaolinite; I/S = mixed-layer illite/smectite; C/S = mixed-layer chlorite/smectite; corr1, corr2, corr4, corr6, corr9 = basal spacing of corrensite; NI = not identified.

The occurrence of corrensite (Figure 3) is restricted to the lower part of the well (depths ≥759 m). The most diagnostic criteria for corrensite are the superlattice peak at 28 to 29 Å, which shifts from 30 to 31 Å when treated with ethylene glycol (EG) and the appearance, after EG solvation, of the (004) reflection at about 7.8 Å (Moore and Reynolds 1989; Weaver 1989). Most glycolated patterns show the following

https://doi.org/10.1346/CCMN.1996.0440513 Published online by Cambridge University Press

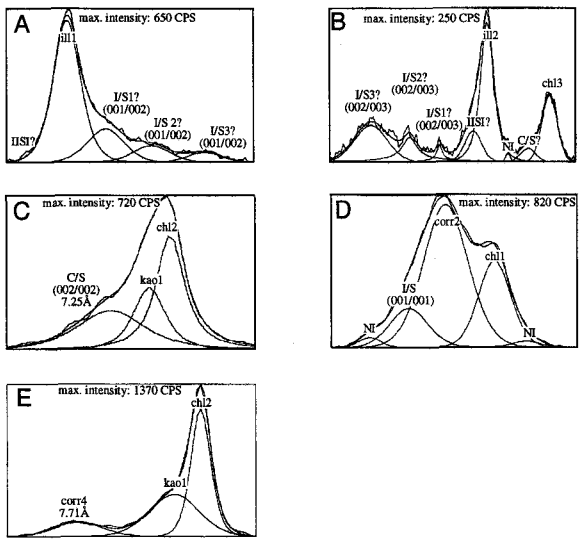

Figure 4. Deconvolution results from different intervals (for location see Figure 3) of samples T84, T456 and T759. Same legend as in Figure 3.

basal reflections of corrensite: (001), (002), (004) and (006).

Kaolinite

Small amounts of kaolinite (Figure 3, for example sample T84) are present throughout the <2 μm fraction (5 to 10%) and in the upper part of the well for the 2 to 16 μm fraction (Figure 2). The relative proportion of kaolinite in the <2 μm fraction remains fairly constant within the studied depth range.

THERMAL MODELING

Primary Input Parameters

The most important problem for the geological reconstruction of the Thônex well is the amount of erosion at the top of the Tertiary. We assume a missing section of 2000 m (Jenny et al. 1995) composed of USM, OMM and OSM deposits for the first simulation runs.

The geothermal regime in peripheral foreland basins is generally characterized as hypothermal, that is to say cooler than normal (Allen and Allen 1990). Typical heat flow values for these basins range from 60 to 80 mW/m^2 (Deming and Chapman 1989; Allen and Allen 1990). Low paleogeothermal gradients (20 to 30 °C/km) have also been reported for the Tertiary of the Molasse basin (Jacob and Kuckelkorn 1977; Rybach 1984; Teichmüller and Teichmüller 1986; Schegg 1994; Jenny et al. 1995). We kept the heat flow history for our model as simple as possible because no firm geological arguments currently exist for any major deviations from normal values during the foreland basin evolution. Therefore, the heat flow was held constant (70 mW/m^2) during the Tertiary with the exception of the Quaternary, where it was increased linearly to the calculated present-day value of 74 mW/m^2.

The variation of the sediment-water and sediment-air interface temperatures during the Tertiary is based on studies by Hochuli (1978).

The petrophysical properties are entirely dependent upon the lithology definition of each modeled formation. The lithologies of drilled formations are based on observations (mud logging, wireline logging) and results from the XRD study, for example whole rock mineralogy and clay mineral composition. Lithologies of eroded formations have been characterized using data from preserved sections in other areas (Matter et al. 1980; Homewood et al. 1986).

Calibration Data

We used 4 different types of calibration data: porosity, temperature, vitrinite reflectance and %Smectite in I/S. Apart from its role as an indicator of the state of compaction, porosity is the most important factor controlling the thermal properties, for example thermal conductivity, of sediments. Porosity values were calculated for 10 sandy horizons in the USM using measured sonic velocities and a standard Schlumberger plot for sandstones. We used the reciprocal relationship of Falvey and Middleton (1981) for the porosity and decompaction computations.

Measured temperatures are only sensitive to thermal perturbations in the relatively recent geological past, and can therefore only be used to calibrate the modern heat flow values. There are no direct temperature measurements in the studied section. A reliable temperature value was measured in Upper Jurassic limestones at a depth of 1900 m, with ground water temperatures at 70 °C. We extrapolated this value to a surface temperature of 9 °C to obtain calibration data in the Molasse section.

Vitrinite reflectance is regarded as one of the most reliable thermal indicators for the calibration of paleoheat flow history (Bustin et al. 1985). Modeled thermal maturity was calculated by the BasinMod program using kinetically-based equations of maturation with time and temperature developed by Sweeney and Burnham (1990). Nine samples from the USM have been analyzed by Jenny et al. (1995) to study the coalification profile of the Thônex well. Vitrinite reflectance values vary from 0.48% Rr (mean random reflectance) in a sample taken at 267 m to 0.71% Rr in a sample taken at 1176 m (Figures 6 and 8). The calculated coalification gradient of 0.18% Rr/km (0.13 log% Rr/km) is rather low and indicative of a "normal" (≈30 °C/km) paleogeothermal gradient (Robert 1985).

According to Pytte and Reynolds (1989), the correlation of I/S composition with temperature and time strongly suggests that the reaction progress is kineti-

https://doi.org/10.1346/CCMN.1996.0440513 Published online by Cambridge University Press

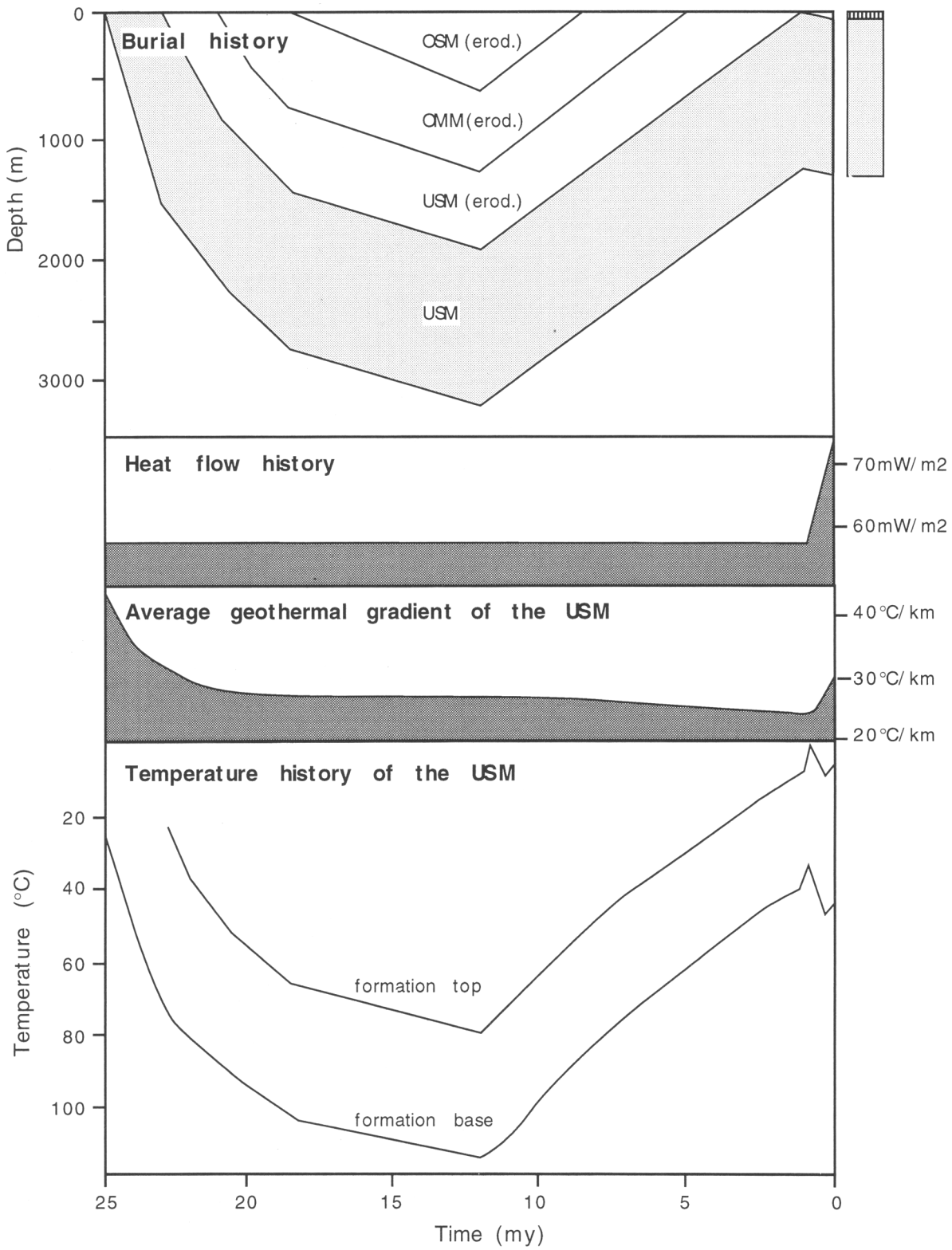

Figure 5. Summary of basin modelling input data and results for the Thônex well. The best-fit calibration was achieved using a constant heat flow of 58 mW/m² during the Tertiary. This results in maximum paleotemperatures of 80 and 115 °C for the top and bottom of the USM section, respectively. The corresponding average geothermal gradient in the Latest Miocene is 27 °C/km.

https://doi.org/10.1346/CCMN.1996.0440513 Published online by Cambridge University Press

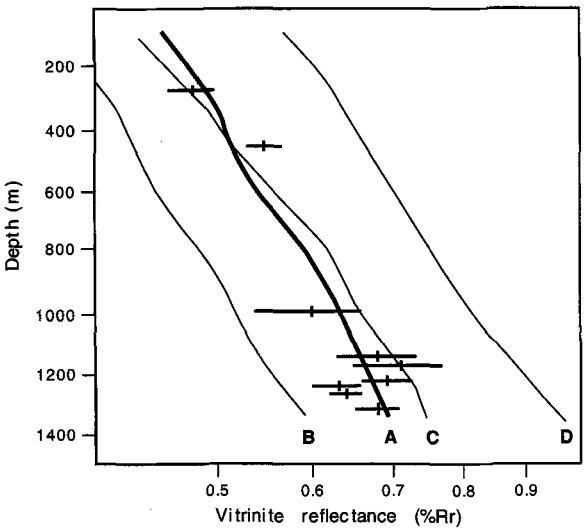

Figure 6. Comparison of 4 models for the calculated vitrinite reflectance profile in the USM section (present-day). A = preferred model with Tertiary heat flow of 58 mW/m² and upper Miocene erosion of 1950 m; B = 58 mW/m² and 1350 m erosion; C = 74 mW/m² and 1350 m erosion; D = 74 mW/m² and 1950 m erosion.

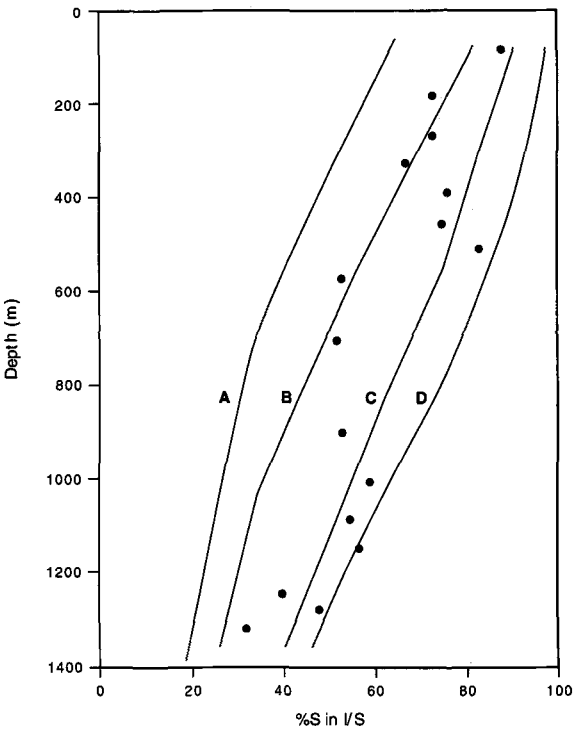

Figure 7. Calculated and measured I/S composition using the kinetic model of Pytte & Reynolds (1989). AE = activation energy (kJ/mol) and FF = frequency factor (s^{-1}). Case A: AE = 138, FF = 5.2×10^7, temperature history of BasinMod; case B: AE = 142, FF = 5.2×10^7, temperature history of BasinMod; case C: AE = 138, FF = 5.2×10^7, temperature history 25% lower than BasinMod; case D: AE = 142, FF = 5.2×10^6, temperature history of BasinMod.

cally controlled. They described the reaction extent by a sixth-order kinetic expression (fifth-order with respect to smectite content and first-order with respect to the K/Na ratio).

Thermal Modeling Results

A Tertiary heatflow value of 58 mW/m² was derived through an iterative approach for the preferred model (Figure 5), which is reasonable for a foreland basin setting with a high sedimentation rate. The resulting average geothermal gradient within the USM section decreases rapidly from more than 40 °C/km to 28 °C/km from 25 to 20 Ma because of the initial rapid compaction (Figure 5). During the whole Miocene, the gradient remained low and decreased to 24 °C/km. Our modeling suggests maximum paleotemperatures of 80 to 115 °C for the USM section during the Late Miocene.

The resulting final model (Figure 5) for the burial and thermal history of the Tertiary section of the Thônex well is in good agreement with most available calibration data, that is, porosity, present-day temperature, vitrinite reflectance and I/S, which are independent of each other.

1) The chosen burial history with a post-Molasse erosion amount of 1950 m results in calculated porosities within the range of 10 to 18%. This is only slightly higher than the range of sonic porosity values of 8 to 17%.

2) Taking into account an uncertainty of ±5 mW/m² (error and low number of measured bottom hole temperatures) the present-day heat flow value fits reasonably well with the regional heat flow map by Bodmer and Rybach (1984).

3) The calculated vitrinite reflectance depth trend compares well with the measured values throughout the USM section (Figure 6, case A).

4) Modeling of the smectite-to-illite transformation with the Pytte and Reynolds (1989) kinetic parameters (activation energy = 138 kJ/mol, frequency factor = 5.2×10^7 s^{-1}) shows that a reasonable fit with the measured values can only be achieved with a temperature history that is approximately 25% lower than the one calibrated by vitrinite reflectance data (Figure 7, compare case A and C; Figure 8, temperature trend B). The kinetic model of the I/S-transformation is highly sensitive to changes in the frequency factor and the activation energy (Figure 7, case B and D).

Sensitivity Analysis

In the thermal model a reduced rate of burial and subsequent erosion might be compensated by an elevated heat flow for the same period. To test the impact of such geological scenarios, a simple sensitivity analysis was carried out. The alternative model (Figure 6,

https://doi.org/10.1346/CCMN.1996.0440513 Published online by Cambridge University Press

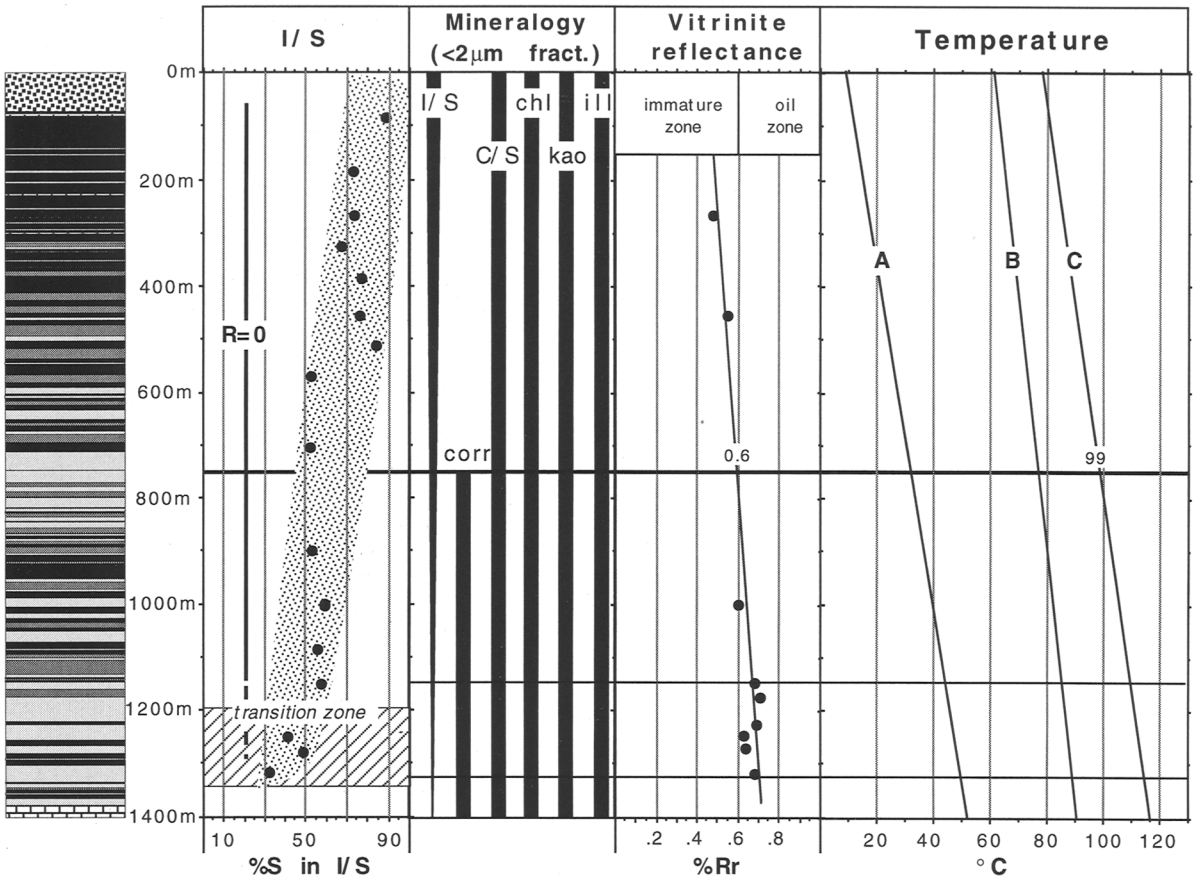

Figure 8. Summary of major inorganic and organic diagenetic changes in the Thônex well and correlation with paleotemperature estimation. A = present-day borehole temperature; B = maximum paleotemperature from I/S simulation with Pytte & Reynolds (1989); C = maximum paleotemperature from thermal modeling with BasinMod. Transition zone = transition from random to ordered I/S (Hoffman and Hower 1979).

case C) with an elevated heat flow of 74 mW/m^2 throughout the Tertiary but a reduced erosion amount (1350 m instead of 1950 m) fits the measured coalification data less than the preferred model. Other model runs resulted in %Rr values that were either consistently lower (Figure 6, case B) or higher (Figure 6, case D) than the measured values.

DISCUSSION

Illite/Smectite

There is a great deal of evidence in the literature indicating the presence of multi-phase clay mineral assemblages. Morphological studies by Inoue et al. (1987, 1988) of the smectite-to-illite conversion revealed the occurrence of three distinct morphologic types of mica-like minerals that appear successively in the illitization process: flakelike crystals identified as random I/S, lathlike and platelike crystals referred to as regularly interstratified I/S. According to Rosenberg et al. (1990), comparison of the inferred chemical compositions of solubility-controlling, mica-like phases with those of apparent phases in natural, hydrothermal materials suggests the existence of 4 illitic layer (ordering) types [S (R0), I/S (R1), ISII ($R \geqq 3$) and I] that behave as discrete, thermodynamic phases. Mixed-layer I/S is regarded as a mixture of one or more of these phases. Based on XRD studies and combined simulation-decomposition approaches for modeling XRD patterns, Lanson and Champion (1991) and Velde and Lanson (1993) postulated multi-phase assemblages in sediments of the Paris Basin. Rettke (1981) attributed the diverse expandability and ordered mixed-layering of the I/S in the Lower Cretaceous Dakota Group shales of the Denver-Julesburg basin to variability within original, unaltered detrital clay. This variability decreased in response to increasing depth and temperature.

A multi-phase I/S assemblage cannot be excluded for the samples studied. Indeed, our deconvolution results could be interpreted in such a way. However, the apparent internal inconsistency, the low intensities of the decomposed peaks and the complexity of our XRD

https://doi.org/10.1346/CCMN.1996.0440513 Published online by Cambridge University Press

patterns (due to the presence of many discrete minerals) leave some serious doubts with this interpretation. Further studies, for example, image analysis or HRTEM, might help to confirm or discard the interpretation of a multi-phase I/S assemblage.

The I/S compositional variation with depth may reflect either errors in the estimate of the expandability, contamination of cuttings from caving of material at shallower depth in the well or some source control.

It is generally agreed that in shales and other low-permeability sediments, diagenetic I/S and illite forms from a smectite or a high expandable I/S precursor. According to Pollastro (1993), any reliable geothermometric interpretation of I/S diagenesis requires that the initial composition of the I/S is known.

Smectite can form by the alteration of volcanic glass, feldspars, micas, various FeMg silicates and silicification of detrital physils (Weaver 1989; p. 153). Given the high amount of feldspar and micas in the USM deposits and the paleoclimatic and paleotopographic conditions (Reggiani 1989), a pedogenic origin of smectite cannot be excluded. The occurrence of smectite and highly expandable I/S in outcrop and near surface samples from the whole Molasse basin support this view (Monnier 1982; Schegg 1992, 1993).

According to Pollastro (1993), the transition from random I/S (R = 0) to ordered I/S (R = 1) roughly coincides with the temperatures generally designated for the beginning of the oil window. Hoffman and Hower (1979) estimate a temperature range of 100 to 110 °C for the ordering change. Pearson and Small (1988) correlate the disappearance of random I/S with a temperature of 93 °C, while Glasmann et al. (1989) found ordering to develop over a temperature range of 80 to 110 °C.

The transition zone (R = 0 to R = 1) in the Thônex well has only been found at the base of the Tertiary at a depth of approximately 1200 to 1300 m (Figure 8). The modeled temperatures for this zone (110 to 115 °C) are only slightly higher than those of the authors mentioned above.

Chlorite/Smectite and Corrensite

Interstratified C/S generally occurs as an intermediate product of the smectite-to-chlorite transformation. A discontinuous decrease in the proportion of smectite in C/S, with steps at smectite-rich C/S, corrensite and chlorite-rich C/S, during the smectite-to-chlorite transformation has been observed in hydrothermal systems and diagenetic environments (Inoue et al. 1984; Inoue and Utada 1991). Reynolds (1988) stated that almost all reported mixed-layer chlorite minerals can be classified into 2 types: nearest order type (R = 1) and randomly interstratified (R = 0) minerals whose compositions lie near one end of the range or the other. The unique chemistry and composition for corrensite implies that it represents a relatively stable phase, intermediate between chlorite and smectite, which is consistent with the occurrence of each of the 3 phases, or mixtures of them, rather than with a complete, continuous sequence of interstratified chlorite and smectite (Shau et al. 1990). Hillier (1995) emphasized that XRD patterns of a R1 ordered chlorite-smectite cannot be distinguished from those involving R0 mixed-layering between corrensite and either smectite or chlorite. The observation that very few XRD studies report C/S with >50% smectite has brought the existence of this mixture into question (Reynolds 1988).

According to Moore and Reynolds (1989), smectite-rich (>70%) S) C/S are characterized by the following peak positions: C/S (001/001) at about 16.4 to 17 Å, C/S (002/002) at approximately 8.4 to 8.2 Å and C/S (004/005) at about 3.4 Å. None of these peaks is present in our samples. We are aware that the (001/001) and the (004/005) peaks, even when using deconvolution techniques, are difficult to identify due to interference with other clay mineral reflections. Conversely, the (002/002) peak should be present because the (001/002) of high expandable I/S (reflections between 8.6 to 8.8 Å, Moore and Reynolds 1989) do not overlap with this phase. Only traces (<20 CPS) of this peak have been observed in a few samples.

Depending upon the geochemical environment, there are different possible pathways by which corrensite may form. Bodine and Madsen (1987) studying an evaporite cycle in the Paradox Basin (Utah) suggested that Mg-smectites may have been the precursor of corrensite and chlorite. Hillier (1993) favored another pathway via reactions between Mg-bearing carbonates and dioctahedral detrital clay minerals in Devonian lacustrine mudrocks. However, most workers agree that a high Mg^{2+}/H^{+} ratio favors the formation of corrensite and chlorite. Such conditions are generally associated with the following sedimentary facies: 1) evaporite; 2) carbonate; 3) basic to intermediate pyroclastic volcanoclastic facies; and 4) greywackes (Kübler 1973). In the Geneva basin, the USM comprises an alternating sequence of 5 basic rock types: sandstone, siltstone, marl, carbonate and gypsum. The association of dolomite and primary gypsum in a dominantly muddy sequence suggests low relief and evaporitic conditions (Reggiani 1989). The sedimentary facies in the Geneva Basin, therefore, favored the formation of corrensite during the diagenesis. Similar observations in wells from the Swiss Molasse Basin have already been made by Monnier (1982). Another likely source for Mg, especially in sandstones of the western Molasse Basin, may be detrital mafic minerals like serpentine (Schegg 1993). From Figure 2 it is apparent that sandstones become more abundant in the lower part of the well. The presence of corrensite may be related, at least in part, to this lithological change.

https://doi.org/10.1346/CCMN.1996.0440513 Published online by Cambridge University Press

In the Thônex well no continuous transformation of smectite-to-chlorite could be observed. The upper part of the well is characterized by chlorite and chlorite-rich C/S, probably of detrital origin. The deeper part of the well (>750 m depth) shows the appearance of corrensite together with discrete chlorite and chlorite-rich C/S. The absence of smectite-rich C/S (>50% smectite) in the upper part of the well may have different reasons: 1) important post-depositional erosion of younger smectite-rich C/S Molasse series; 2) XRD identification problems; or 3) no trioctahedral smectite in the initial sediment, for example formation of corrensite without a smectite precursor (Hillier 1993).

Kübler (1973) suggested that trioctahedral corrensite is an indicator of diagenetic temperatures of 90 to 100 °C. This temperature range has been modified somewhat by more recent authors. The temperature for the first appearance of corrensite has been estimated as 100 °C in Miocene volcanoclastic rocks of Japan by Inoue and Utada (1991), 70 °C in shales and 60 °C in sandstones by Chang et al. (1986) and 80 °C in sandstones by Hoffman and Hower (1979). In the Thônex well, corrensite appears at an inferred paleotemperature of about 100 °C. This is in line with observations by Kübler (1973) and Inoue and Utada (1991).

Thermal Modeling

Thermal modeling results from the Thônex well suggest a Tertiary heat flow of 58 mW/m^2 and a geothermal gradient of 27 °C/km during maximum burial. Such low geothermal gradients and heat flow values during the Tertiary have also been observed for other wells from the Swiss and German Molasse Basin (Rybach and Bodmer 1980; Schegg 1994; Jenny et al. 1995; Teichmüller and Teichmüller 1986). The increase of the thermal gradient during the Quaternary has no infuence on the vitrinite reflectance or I/S evolution within the studied section. It is either related to inherent calculation problems of the present-day heat flow (defined thermal conductivities are too low) or to real short-term thermal perturbations. Such heat flow fluctuations may be caused by local fluid circulation in the vicinity of regional deep-reaching fracture zones, for example Arve strike-slip zone (Figure 1), similar to the well-documented heat flow anomalies of northern Switzerland (Schärli and Rybach 1991). The variations in the most recent temperature history (Figure 5) are to some extent related to the variations in surface temperature during the Quaternary glacial periods.

The calibrated post-Molasse erosion amount of 1950 m is in agreement with similar regional studies in the Molasse Basin (Lemcke 1974; Monnier 1982; Schegg 1993).

The simulation of the smectite-to-illite transformation with the kinetic model of Pytte and Reynolds (1989) showed the difficulties when using I/S data as a calibration tool. The kinetic model seems to be very sensitive to small changes in the kinetic parameters. The observed disagreements, however, may be the result of an incomplete understanding of clay mineral transformation processes and the lack of reliable kinetic data (Velde and Vasseur 1992). As a consequence, we could not use the I/S data as reliable calibration data.

CONCLUSIONS

The major results of this study are summarized in Figure 8.

Clay Mineral Diagenesis

1) The bulk rock composition lacks systematic variation with depth. Dominant mineral phases are quartz, calcite and phyllosilicates. K-feldspar, plagiclase, gypsum, anhydrite and dolomite are minor constituents.

2) Discrete illite, chlorite and kaolinite are present (2 to 16 μm and <2 μm fraction) over the entire studied section and regarded as detrital.

3) The major diagenetic changes are the decrease of expandability of I/S from approximately 90 to 30% smectite layers with depth, the decrease in abundance of I/S in the clay mineral fraction and the appearance of corrensite at depths >750 m.

Correlation of Thermal Indicators and Paleotemperatures

1) The transition from random I/S to ordered I/S is associated with coal ranks of approximately 0.7% Rr and corresponding paleotemperatures at 110 to 115 °C.

2) Corrensite appears at a vitrinite reflectance value of 0.6% Rr and a corresponding paleotemperature of approximately 100 °C.

Thermal Modeling

1) Kinetic modeling of vitrinite reflectance data suggests geothermal gradients for the time of maximum burial (late Miocene) of approximately 27 °C/km. This is less than the observed present-day gradient of 31.2 °C/km.

2) A calibrated post-Molasse erosion amount of 1950 m has been obtained. This is in agreement with similar regional studies in the Molasse Basin (Lemcke 1974; Monnier 1982; Schegg 1993).

3) Thermal modeling of the Thônex well results in a constant Tertiary heat flow of 58 mW/m^2 and maximum paleotemperatures for the USM section of 80 to 115 °C during maximum burial in the Late Miocene.

4) Modeling of the smectite-to-illite transformation using the Pytte and Reynolds (1989) kinetic parameters shows, that a reasonable fit to measured values could only be achieved using a temperature history that is about 25% lower than the one calibrated using vitrinite reflectance. Such disagreements, however, may be the result of incomplete understanding of clay

https://doi.org/10.1346/CCMN.1996.0440513 Published online by Cambridge University Press

mineral transformation processes and the lack of reliable kinetic parameters.

ACKNOWLEDGMENTS

This research was funded by the Swiss National Foundation for Scientific Research (project No. 2000-037585.93/1). We are indebted to J. Jenny and J.-P. Burri (Géologie-Géophysique, Geneva), the Geneva Canton Department of Energy (OCEN), the Swiss Federal Department of Energy (OFEN) for providing samples and data. We are grateful to journals reviewers S. Hillier (Aberdeen), C. Spötl (Innsbruck) and J. Matyas (Bern) for their constructive criticisms. For practical support, helpful contributions or critical review of the manuscript we would like to thank the following: T. Adatte (Neuchâtel), S. Altaner (Urbana), D. Fraser (Oxford), M. Frey (Basel), B. Kübler (Neuchâtel), J. Uriarte (Geneva) and W. Wildi (Geneva).

REFERENCES

Allen PA, Allen JR. 1990. Basin analysis: Principles and applications. Oxford: Blackwell Scientific Publication. 451 p.

Berger J-P, Charollais J, Hugueney M. 1987. Nouvelles données biostratigraphiques sur la Molasse rouge du bassin genevois. Arch Sci Genève 40:77–95.

Bodine MW, Jr, Madsen BM. 1987. Mixed-layer chlorite/smectites from a Pennsylvanian evaporite cycle, Grand County, Utah. In: Schultz LG, van Olphen H, Mumpton FA, editors. Proceeding of the International Clay Conference Denver. Boulder, CO: The Clay Minerals Society. p 85–93.

Bodmer P, Rybach L. 1984. Geothermal map of Switzerland (heat flow density). Beitr Geol Schweiz, Ser Geophysik 22. 47 p.

Bustin RM, Barnes MA, Barnes WC. 1985. Diagenesis 10. Quantification and modelling of organic diagenesis. Geosci Canada 12:4–21.

Chang HK, Mackenzie FT, Schoonmaker J. 1986. Comparison between the diagenesis of dioctahedral and trioctahedral smectite, Brazilian offshore basins. Clays Clay Miner 34:407–423.

Deming D, Chapman DS. 1989. Thermal histories and hydrocarbon generation: An example from the Utah-Wyoming thrust belt. Bull Am Assoc Petrol Geol 73:1455–1471.

Falvey DA, Middleton MF. 1981. Passive continental margins: Evidence for prebreakup deep crustal metamorphic subsidence mechanism. In: Proceedings 26th International Geological Congress, Geology of continental margins symposium. Paris: Oceanologica Acta. p 103–114.

Glasmann JR, Larter S, Briedis NA, Lundegard PD. 1989. Shale diagenesis in the Bergen High Area, North Sea. Clays Clay Miner 37:97–112.

Gorin G, Signer C, Amberger G. 1993. Structural configuration of the western Swiss Molasse Basin as defined by reflection seismic data. Eclogae Geol Helv 86:693–716.

Hillier S. 1993. Origin, diagenesis, and mineralogy of chlorite minerals in Devonian lacustrine mudrocks, Orcadian Basin, Scotland. Clays Clay Miner 41:240–259.

Hillier S. 1995. Mafic phyllosilicates in low-grade metabasites. Characterization using deconvolution analysis—Discussion. Clay Miner 30:67–73.

Hochuli PA. 1978. Palynologische Untersuchungen im Oligozän und Untermiozän der Zentralen und Westlichen Paratethys. Beitr Paläont Oesterreich 4:1–132.

Hoffman J, Hower J. 1979. Clay mineral assemblages as low grade metamorphic geothermometers: Application to the thrust faulted disturbed belt of Montana, USA. SEPM Spec Publ 26:55–79.

Homewood P, Allen PA, Williams GD. 1986. Dynamics of the Molasse Basin of western Switzerland. Spec Publ Int Assoc Sediment 8:199–217.

Inoue A, Utada M, Nagata H, Watanabe T. 1984. Conversion of trioctahedral smectite to interstratified chlorite/smectite in Pliocene acidic pyroclastic sediments of the Ohyu district, Akita prefecture, Japan. Clay Sci Soc Japan 6:103–116.

Inoue A, Kohyama N, Kitagawa R, Watanabe T. 1987. Chemical and morphological evidence for the conversion of smectite to illite. Clays Clay Miner 35:11–120.

Inoue A, Velde B, Meunier A, Touchard G. 1988. Mechanism of illite formation during smectite-to-illite conversion in a hydrothermal system. Am Mineral 73:1325–1334.

Inoue A, Utada M. 1991. Smectite-to-chlorite transformation in thermally metamorphosed volcanoclastic rocks in the Kamikita area, northern Honshu, Japan. Am Mineral 76: 628–640.

Jacob H, Kuckelkorn K. 1977. Das Inkohlungsprofil der Bohrung Miesbach 1 und seine erdölgeologische Interpretation. Erdöl-Erdgas-Z 93:115–124.

Jenny J, Burri J-P, Muralt R, Pugin A, Schegg R, Ungemach P, Vuataz F-D, Wernli R. 1995. Le forage géothermique de Thônex (Canton de Genève): aspects stratigraphiques, tectoniques, diagénétiques, géophysiques et hydrogéologiques. Eclogae Geol Helv 88:365–396.

Kisch HJ. 1987. Correlation between indicators of very low-grade metamorphism. In: Frey M, editor. Low temperature metamorphism. Glasgow-London: Blackie. p 227–300.

Kübler B. 1973. La corrensite, indicateur possible de milieux de sédimentation et du degré de transformation d'un sédiment. Bull Cent Rech-Expl Elf-Aquitaine, Pau-SNPA 7: 543–556.

Lanson B, Champion D. 1991. The I/S-to-illite reaction in the late stage of diagenesis. Am J Sci 291:473–506.

Larter S. 1989. Chemical models of vitrinite reflectance evolution. Geol Rdsch 78:349–359.

Laubscher HP. 1974. Basement uplift and decollement in the Molasse Basin. Eclogae Geol Helv 67:531–537.

Lemcke K. 1974. Vertikalbewegungen des vormesozoischen Sockels im nördlichen Alpenvorland vom Perm bis zur Gegenwart. Eclogae Geol Helv 67:121–133.

Matter A, Homewood P, Caron C, Van Stuijvenberg J, Weidmann M, Winkler W. 1980. Flysch and Molasse of western and central Switzerland. In: Trümpy R, editor. Geology of Switzerland: A guide book. Part B: Geological excursions. Basel-New York: Schweiz Geolog Kommission, Wepf and Co Publishers. p 261–293.

Monnier F. 1982. Thermal diagenesis in the Swiss molasse basin: Implications for oil generation. Can J Earth Sci 19: 328–342.

Moore DM, Reynolds RC. 1989. X-ray diffraction and the identification and analysis of clay minerals. Oxford-New York: Oxford University Press. 322 p.

Pearson MJ, Small JS. 1988. Illite-smectite diagenesis and palaeotemperatures in northern North Sea Quaternary to Mesozoic shale sequences. Clay Miner 23:109–132.

Pfiffner AO. 1986. Evolution of the north Alpine foreland basin in the Central Alps. Spec Publs Int Assoc Sediment 8:219–228.

Pollastro RM. 1993. Considerations and applications of the illite/smectite geothermometer in hydrocarbon-bearing rocks of Miocene to Mississippian age. Clays Clay Miner 41:119–133.

Pollastro RM, Barker CE. 1986. Application of clay-mineral, vitrinite reflectance, and fluid inclusion studies to the thermal and burial history of the Pinedale anticline, Green River Basin, Wyoming. SEPM Spec Publ 38:73–83.

https://doi.org/10.1346/CCMN.1996.0440513 Published online by Cambridge University Press

Pytte AM, Reynolds RC. 1989. The thermal transformation of smectite to illite. In: Naeser ND and McCulloh TH, editors. Thermal history of sedimentary basins: Methods and case histories. New York-Berlin-London-Paris-Tokyo: Springer-Verlag. p 133–140.

Reggiani L. 1989. Faciès lacustres et dynamique sédimentaire dans la Molasse d'eau douce inférieure Oligocène (USM) de Savoie. Eclogae Geol Helv 82:325–350.

Renac C, Meunier A. 1995. Reconstruction of palaeogeothermal conditions in a passive margin using illite-smectite mixed-layers series (BA1 scientific drill-hole, Ardeche, France). Clay Miner 30:107–118.

Rettke RC. 1981. Probable burial diagenetic and provenance effects on Dakota Group clay mineralogy, Denver Basin. J Sed Petrol 51:541–551.

Rey J-Ph, Kübler B. 1983. Identification des micas des séries sedimentaires par diffraction X à partir de la série harmonique (001) des préparations orientées. Schweiz mineral petrogr Mitt 63:13–36.

Reynolds RC. 1985. NEWMOD© a computer program for the calculation of one-dimensional diffraction patterns of mixed-layer clays. RC Reynolds, 8 Brook Rd., Hanover, New Hampshire, USA.

Reynolds RC. 1988. Mixed layer chlorite minerals. In: Bailey SW, editor. Hydrous phyllosilicates (exclusive of micas). Reviews in Miner 19:601–630.

Robert P. 1985. Histoire géothermique et diagenèse organique. Mém Centres Rech Expl-Prod Elf-Aquitaine 8:345 p.

Rosenberg PE, Kittrick JA, Aja SU. 1990. Mixed-layer illite/smectite: A multiphase model. Am Mineral 75:1182–1185.

Rybach L. 1984. The paleogeothermal conditions of the Swiss molasse basin: implication for hydrocarbon potential. Rev Inst franç Pétrole 39:143–146.

Rybach L, Bodmer P. 1980. Die geothermischen Verhältnisse der Schweizer Geotraverse im Abschnitt Basel-Luzern. Eclogae Geol Helv 73:501–512.

Schärli U, Rybach L. 1991. Geothermische Detailkartierung der zentralen Nordschweiz 1:100'000. Beitr Geol Schweiz, Ser Geophysik 24:51 p.

Schegg R. 1992. Coalification, shale diagenesis and thermal modelling in the Alpine Foreland basin: the Western Molasse basin (Switzerland/France). Org Geochem 18:289–300.

Schegg R. 1993. Thermal maturity and history of sediments in the North Alpine Foreland Basin (Switzerland, France). Geneva: Université de Genève, Publ du Département de Géologie et Paléontologie 15:194 p.

Schegg R. 1994. The coalification profile of the well Weggis (Subalpine Molasse, Central Switzerland): Implications for erosion estimates and the paleogeothermal regime in the external part of the Alps. *Bull Vereinigung schweiz* Petroleum-Geol und -Ing 61:57–67.

SCINTAG®. 1992. Users manual, version 2.15, 230 p.

Shau Y-H, Peacor DR, Essene EJ. 1990. Corrensite and mixed-layer chlorite/corrensite in metabasalt from northern Taiwan: TEM/AEM, EMPA, XRD, and optical studies. Contrib Miner Petrol 105:123–142.

Smart G, Clayton T. 1985. The progressive illitization of interstratified illite-smectite from Carboniferous sediments of northern England and its relationship to organic maturity indicators. Clay Miner 20:455–466.

Sweeney JJ, Burnham AK. 1990. Evaluation of a simple model of vitrinite reflectance based on chemical kinetics. Bull Am Assoc Petrol Geol 74:1559–1570.

Teichmüller R, Teichmüller M. 1986. Relations between coalification and palaeogeothermics in Variscan and Alpidic foredeeps of western Europe. In: Buntebarth G, Stegena L, editors. Paleogeothermics. Berlin-Heidelberg-New York-London-Paris-Tokyo: Springer-Verlag. Lecture Notes in Earth Sci 5:53–78.

Tissot BP, Pelet R, Ungerer Ph. 1987. Thermal history of sedimentary basins, maturation indices and kinetics of oil and gas generation. Bull Am Assoc Petrol Geol 71:1445–1466.

Velde B, Lanson B. 1993. Comparison of I/S transformation and maturity of organic matter at elevated temperatures. Clays Clay Miner 41:119–133.

Velde B, Vasseur G. 1992. Estimation of the diagenetic smectite to illite transformation in time-temperature space. Am Mineral 77:967–976.

Weaver CE. 1989. Clays, muds, and shales. Amsterdam-Oxford-New York-Tokyo: Elsevier. Developments in Sedimentology 44:819 p.

Wildi W, Huggenberger P. 1993. Reconstitution de la plateforme européenne anté-orogénique de la Bresse aux Chaînes subalpines; éléments de cinématique alpine (France et Suisse occidentale). Eclogae Geol Helv 86:47–64.

(Received 23 August 1995; accepted 13 February 1996; Ms. 2682)

https://doi.org/10.1346/CCMN.1996.0440513 Published online by Cambridge University Press